Hydrodynamic stability theory and wall turbulence

P. K. Sen and Srinivas V. Veeravalli*

Department of Applied Mechanics, Indian Institute of Technology, New Delhi 110 016, India

This paper discusses the role of hydrodynamic stability theory in understanding wall bounded turbulent flows. Work in this area was pioneered by Malkus, followed by Reynolds and Tiederman and Reynolds and Hussain. The experimental results, and theoretical cum computational results of Reynolds and Hussain, were significant in many ways. Mainly, they highlighted the behaviour of organized disturbances introduced into the flow field. However, no conclusions could be reached, one way or other, regarding a definite connection between hydrodynamic instability and wall turbulence. More recently, and over the past few years, we have improved upon the theoretical analysis of Reynolds and Hussain and have also done some experiments. We are now able to conclude much more positively that organized disturbances and hydrodynamic instability modes may have a very definite connection with wall turbulence. Here we present brief reviews of the past works of others and mainly summarize our work and discuss some of our recent findings.

Introduction

Hydrodynamic stability theory, and several of the theoretical and numerical results based on this theory, have been a fascinating subject of study over the past several decades. These results, and the experiments inspired by them, have led to virtually the entire body of knowledge that exists today on laminar to turbulent transition.

In a relatively limited context, though not any less significant than the topic of laminar-turbulent transition, the question has been asked as to whether or not there is any connection between *hydrodynamic instability and actual turbulence itself*. The answers obtained in the past have been fairly mixed, but the work of the present authors over the past few years seems at least to keep the question alive. Let us take a brief look at the past work on this subject.

One very significant statement that can be made is that hydrodynamic stability theory does indeed have a *strong presence in free turbulent shear flows*. In fact the dominant coherent structure in free turbulent shear flow is the *inviscid instability of the (turbulent) mean- velocity profile*, which is inflectional in the cases of free turbulent shear flows. Amongst a number of results confirming this, the work of Gaster *et al.*[1] on the turbulent mixing layer is a good example. There is also a comprehensive review on stability and free turbulent shear flows by Liu[2], and a more recent overview by Roshko[3]. Where this question remains ambivalent however, is in *wall-turbulent flows*.

The question of a connection between stability theory and turbulent shear flow was first raised by Landau[4] based on a non-linear stability model. Whilst his work did not prove to be a suitable model for turbulence, his equation for non-linear growth found many applications in the field of instability and transition. The next work of great conceptual importance is that of Malkus[5], wherein a theory of turbulence was developed based on the concept, of marginal stability. According to this concept, it was proposed that if the mean velocity profile typical of wall bounded turbulent flows is used in the solution of the classical Orr-Sommerfeld equation, then the profile would prove to be marginally or neutrally stable at the existing flow Reynolds number. It is significant also that Malkus suggested that the *molecular viscosity* and not the eddy viscosity be used in the solution of the Orr-Sommerfeld equation. Malkus's theory was rigorously put to test in an important work by Reynolds and Tiederman[6]. This work also gives a lucid review of Malkus's theory. Reynolds and Tiederman[6] investigated the stability of fully developed turbulent flow between parallel plates, on the lines of Malkus's proposed theory. They used the turbulent mean velocity profile for channel flow in the solution of the classical Orr-Sommerfeld equation (using the molecular viscosity in the equation). The results obtained showed without doubt that Malkus's theory as proposed was not valid, and there was a huge discrepancy between the flow Reynolds number and the Reynolds number corresponding to neutral or marginal stability, the latter being an order of magnitude higher than the former. Prabhu (1967, pers. commun.) also independently obtained the same result. More recently, Sen *et al.*[7] obtained the same result for the turbulent boundary layer flow problem.

The general question of connection between instability and turbulence, with reference to wall bounded turbulent shear flow, went through another round of serious examination by Reynolds and Hussain[8]. This time, abandoning Malkusian precepts, first the basic equations were derived for a superposed organized dis-

*For correspondence. (e-mail: svrvalli@am.iitd.ernet.in)

We dedicate this paper to Prof. Satish Dhawan and pay our humble tribute to this great savant, who is the doyess of researchers in the field of laminar to turbulent transition in our country.

turbance in turbulent flow. Thereafter an equation for the stability of this organized disturbance was derived, which was like an augmented form of the classical Orr-Sommerfeld equation, but containing extension terms dependent on the *eddy viscosity*. Underlying the model was a closure problem for the Reynolds stress tensor, which was resolved based on what the authors called the 'Newtonian eddy' model. Results of solution of their extended Orr-Sommerfeld equation, for channel flow, again yielded damped modes. Nevertheless, the results were closer to establishing a connection between instability and turbulent wall flows than was obtained in ref. 6. Experiments performed by Hussain and Reynolds[9,10] showed some agreement with the theory of Reynolds and Hussain[8]. Subsequently, some non-linear and three-dimensional theories were also developed[11], but these are outside the scope of present discussions.

The present authors have re-examined the question of the connection between instability and wall turbulence, and have obtained an improved theoretical model for the problem. Experiments performed also confirm the theoretical findings. So far as theory is concerned, the chief improvement over Reynolds and Hussain[8] is that a more realistic and improved model has been chosen for the turbulent stress tensor, based on the anisotropic model of Pope[12]. This model gives further extensions of the Orr-Sommerfeld equation over what Reynolds and Hussain[8] obtained. The results show that an unstable wall-mode exists over a wide range of the spatial wave number α. The instability characteristics scale very well with the inner variables of turbulent flow, and are virtually independent of the outer conditions. Therefore the results are quite universal for wall turbulence and depend little on the specific geometry of the problem. Extensive numerical computation has been done, for the cases of turbulent boundary-layer, as well as channel flow, to confirm this. One of the interesting theoretical findings is that *the organized disturbances mimic some of the key features of wall-turbulence*.

Some experiments have also been performed which are reported in Sen and Veeravalli[16]. The one-dimensional energy spectrum, for the turbulent longitudinal velocity, indicates that the range of unstable wavelengths is well contained within the energy-containing part of the energy spectrum. More recently, experiments have also been performed by the present authors to compare the theoretical and experimental eigenfunctions, corresponding to the organized disturbances. Good confirmation is obtained for the proposed theory, from the experimental results. These experiments are discussed later on in the present paper.

Thus, the results obtained so far, both theoretical and experimental, keep alive the question of relevance of stability theory in understanding turbulence in wall-bounded turbulent flows.

Details of past work by the authors may be seen in refs 13–19.

Theory

The instantaneous velocity vector u_i obeys the Navier–Stokes and continuity equations:

$$\frac{\partial u_i}{\partial t} + u_j \frac{\partial u_i}{\partial x_j} = -\frac{1}{\rho}\frac{\partial p}{\partial x_i} + \nu \frac{\partial^2 u_i}{\partial x_j \partial x_j}, \tag{1a}$$

$$\frac{\partial u_i}{\partial x_i} = 0. \tag{1b}$$

The velocity and pressure fields are decomposed in turbulent flows by the well-known Reynolds decomposition; typically,

$$u_i = \overline{u}_i + u_i'; \quad p = \overline{p} + p'. \tag{2}$$

Here $\overline{u}_i, \overline{p}$ are respectively the mean velocity and pressure, and u'_i, p' are the (random) turbulent fluctuations. If we now superpose an organized (solenoidal) disturbance $\tilde{u}_i, \tilde{p}$ (with zero mean), the instantaneous velocity and pressure are respectively given as follows:

$$u_i = \overline{u}_i + \tilde{u}_i + u_i'; \quad p = \overline{p} + \tilde{p} + p'. \tag{3a}$$

The time averages of u_i, p are still respectively $\overline{u}_i, \overline{p}$, but, the ensemble (phase locked) averages

$$\langle u_i \rangle = \overline{u}_i + \tilde{u}_i, \quad \langle p \rangle = \overline{p} + \tilde{p}, \tag{3b}$$

are different. Moreover, the organized disturbance is assumed small, or linear, and in addition it obeys the following:

$$|\langle \tilde{u}_i \tilde{u}_j \rangle| \ll |\langle u_i' u_j' \rangle|. \tag{4}$$

The above assumption (4) restricts the organized disturbances to being weaker than what was considered by Reynolds and Hussain[8].

For future clarity some definitions and notations are introduced: (i) an overbar (–) over any quantity will imply time average; (ii) the symbols $\langle\ \rangle$ enclosing a quantity will imply ensemble average. After some algebra, described in Sen and Veeravalli[16], one is in a position to obtain the dynamic equation for the organized disturbance,

$$\frac{\partial \tilde{u}_i}{\partial t} + \overline{u}_j \frac{\partial \tilde{u}_i}{\partial x_j} + \tilde{u}_j \frac{\partial \overline{u}_i}{\partial x_j} = -\frac{1}{\rho}\frac{\partial \tilde{p}}{\partial x_i} + \nu \frac{\partial^2 \tilde{u}_i}{\partial x_j \partial x_j} + \frac{\partial \tilde{r}_{ij}}{\partial x_j}, \tag{5}$$

where $\tilde{r}_{ij}$ is the modulation in the Reynolds stress tensor, given by

$$\tilde{r}_{ij} \equiv -(\langle u_i' u_j' \rangle - \overline{u_i' u_j'}). \quad (6)$$

Reynolds and Hussain[8] have shown that $\tilde{r}_{ij} \sim O(\tilde{u}_i)$. The above equations pose a closure problem for the various forms of the turbulent stresses, including for $\tilde{r}_{ij}$. It will be instructive to look at simplified physical models and reasoning to understand the manner of resolution proposed for the closure problems.

At this stage we introduce (twice) the rate of strain tensor and (twice) the vorticity tensor, respectively s_{ij} and ω_{ij}, as follows:

$$s_{ij} = \left(\frac{\partial u_i}{\partial x_j} + \frac{\partial u_j}{\partial x_i} \right); \quad \omega_{ij} = \left(\frac{\partial u_i}{\partial x_j} - \frac{\partial u_j}{\partial x_i} \right). \quad (7a, b)$$

These expressions are in generic form, implying that if for example u is replaced by $\overline{u}$, then s_{ij} and ω_{ij} are respectively replaced by $\overline{s}_{ij}$ and $\overline{\omega}_{ij}$.

Attention is restricted to 2-D parallel and near-parallel mean-flows, specifically the turbulent boundary-layer and channel flow. Definition sketches of the two problems are shown in Figure 1 *a*, *b*. Note that in the discussions to follow, the vectors (u_1, u_2, u_3) and (u, v, w) will be used interchangeably and so also (x_1, x_2, x_3) and (x, y, z). The x coordinate is in the direction of the free stream, y is in the direction normal to the wall, and z is the transverse direction. Also we make the quasi-parallel assumption due to which the mean-velocity field is given as $\overline{u} = \overline{u}(y)$, $\overline{v} \approx 0$, and $\overline{w} = 0$. Further, all the mean-velocity gradients, except for $\partial\overline{u}/\partial y$, are either zero, or negligibly small. The turbulence (u_i')-field is also assumed homogeneous in the z direction, and near homogeneous in the x direction. All derivatives of time-averaged quantities are zero in the z-direction, and nearly zero in the x-direction. Moreover the correlations $\overline{u'w'}$ and $\overline{v'w'}$ are zero. However, $\overline{w'^2}$ is non-zero, and this term keeps the Reynolds stress tensor $\overline{u_i' u_j'}$ as three dimensional. The outer velocity scale for the boundary-layer flow problem is the free stream velocity, U_∞, and for the channel flow problem it is the sectional average velocity V. The outer length scale for the boundary layer problem is the boundary layer thickness δ or the displacement thickness δ^*. For the channel flow problem it is the half width of the channel H. Both the problems have the *same* inner scalings, namely friction velocity, v^* as the velocity scale and with ν/v^* as the inner length scale. The characteristic Reynolds number for the problems are respectively $R = U_\infty \delta/\nu$ for boundary layer flow, and $R = VH/\nu$ for channel flow.

One needs now to look at the closure problem for the modulation Reynolds stress tensor $\tilde{r}_{ij}$. Much of the physics of this problem is described in ref. 16. The salient points are that, so long as organized disturbances are small compared to the random disturbances, the problem continues to be defined by the Generalized Eddy Viscosity Hypothesis (GEVH), in which the turbulence

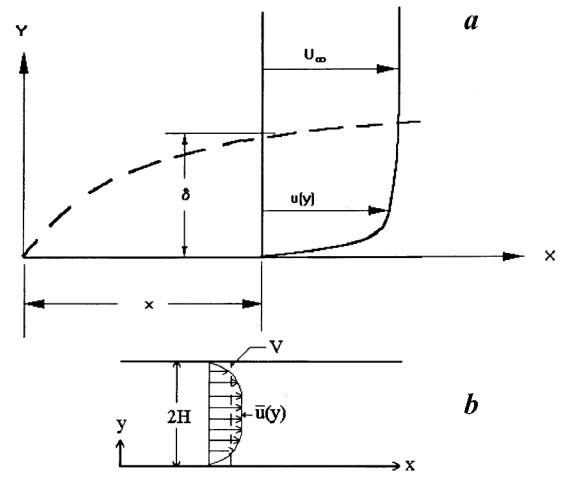

Figure 1. ***a***, Definition sketch for the flat-plate turbulent boundary-layer; ***b***, Definition sketch of the channel flow.

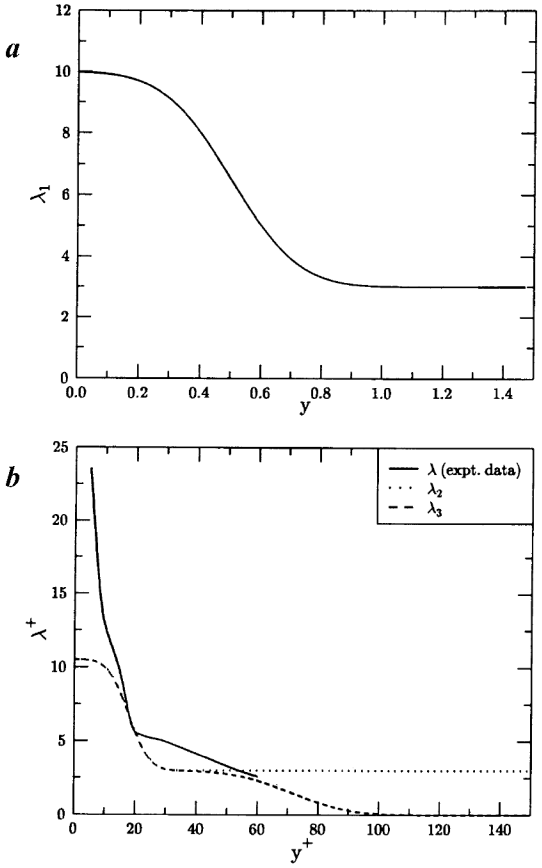

Figure 2. ***a***. Graph of anisotrophy function (from expression for λ_1) versus y (= y_d/δ), standardized in terms of outer variables; ***b***, Graph of anisotropy function λ^+ (= λ) versus y^+, standardized in terms of inner variables. Comparison of the anisotropy function based on experimental data of Klebanoff, and expressions λ_2 and λ_3.

problem is described by *one* length scale and *one* velocity scale. Further the turbulent and mean flow time scales are comparable. Under GEVH, therefore, the stress tensor can be described by appropriate generalized tensorial combinations of turbulence-related quantities and mean flow gradients. In order to improve over the formulation of Reynolds and Hussain[8], it was found expedient to use an 'anisotropic eddy viscosity model' based on the model proposed by Pope[12]. This model is

$$-\overline{u_i'u_j'} = -\frac{2}{3}k\delta_{ij} + \varepsilon\bar{s}_{ij} - \varepsilon\left(\frac{\lambda}{(\bar{u})'}\right)\left[\frac{1}{2}[\bar{\omega}_{ik}\bar{s}_{kj} - \bar{s}_{ik}\bar{\omega}_{kj}]\right], \tag{8}$$

where $k \equiv \frac{1}{2}(\overline{u_i'u_j'})$ is the turbulence kinetic energy, and two empirical functions are introduced, namely the eddy viscosity ε and the so-called 'anisotropy function' λ. Both these quantities require some description. But prior to that, it is instructive to note that the *tensorial form* of equation (8), as shown by Pope[12], is quite unique; only the defining constants, or scalar functions like ε and λ, need to be determined from matching with experimental data. Thus, equation (8) is a significant, consistent and also *tensorially unique* improvement over the isotropic eddy viscosity model, which is obtained by putting $\lambda = 0$ in (8).

Details of the eddy viscosity, also defined in non-dimensional form as $E = \varepsilon/\nu$, may be seen in ref. 16. Basically, in the *inner region*, E scales with inner variables and is universal. In the outer region the shape of E is problem specific, like whether channel flow or boundary layer flow is being considered, and the magnitude of E depends on the flow Reynolds number (based on outer variables).

The anisotropy function λ is formally defined as $\lambda = C(k/(-\overline{u'v'}))$, where C is a constant that needs to be matched from experimental data. Details of the matching procedure are discussed in ref 16. As may be seen from (8) above, if $\lambda \equiv 0$, then all the *normal stress components* $\overline{u'^2}, \overline{v'^2}$ and $\overline{w'^2}$ are identical and equal to $\frac{2}{3}k$. Surely such a model is gravely in error close to the wall where these quantities are very different from each other. With λ non-zero, it is seen from (8) that the normal stress components can be made unequal. Thus, by matching from experimental data λ may be suitably back-calculated.

Generally speaking, two features are salient in the empirical definition of λ, namely it has a high value (around 10) near the wall and tapers off to a low value and finally to zero in the outer region. Thus, the most 'comfortable' shape of λ, from the viewpoint of (easing of) stiffness of the numerical calculations for stability, is shown in Figure 2 *a*. The algebraic details are given in ref. 16. This particular form, called $\lambda = \lambda_1$, basically is written in outer variable form. The high value persists till about mid range in y, and is made to taper off towards the boundary layer edge/channel centerline.

Two other forms of λ, namely λ_2 and λ_3 are shown in Figure 2 *b*. This figure also shows the actual back-calculated value of λ from experimental data. Based on this experimental plot two other empirical forms of λ, namely λ_2 and λ_3, were obtained and used in the calculations. The detailed expressions may be seen in refs 16, 19. Essentially, λ_2 and λ_3 are based on inner variables, and are identical till about $y^+ = 50$, after which λ_2 is made to attain a constant value of 3; whilst λ_3 is tapered off to 0 in the outer region. As will be seen later, the stability calculations are not much affected by the assumed form of λ, especially for the inner modes. However λ_3 is the best overall choice, as the same expression can be used for capturing inner and outer modes. Besides, λ_3 is more faithful to the experimental data also.

We now proceed further with the formulation. Using some arguments discussed in detail in ref. 16, the same form as (8) may also be proposed for $\langle u_i'u_j'\rangle$. The salient points are that (i) the presence of organized disturbances does not modify turbulence-related quantities like the eddy viscosity; and (ii) the organized disturbances *do modulate the mean-flow*, as may be seen from (3 *a*, *b*). Thus one obtains

$$-\langle u_i'u_j'\rangle = -\frac{2}{3}k\delta_{ij} + \varepsilon\langle s_{ij}\rangle - \varepsilon\left(\frac{\lambda}{(\bar{u})'}\right) \times\left[\frac{1}{2}[\langle\omega_{ik}\rangle\langle s_{kj}\rangle - \langle s_{ik}\rangle\langle\omega_{kj}\rangle]\right]. \tag{9}$$

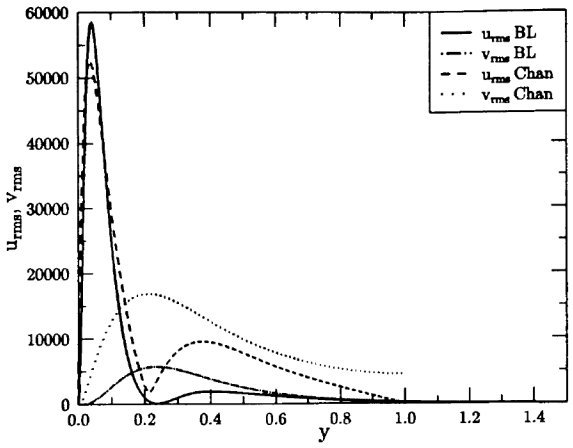

Figure 3. Graph for rms values of u and v versus y. Normalization, $\phi = 1 + 0i$ at $y = 1.0$ for channel flow and, $R = 5000$, $\alpha = 3.15$, $c_r = 0.3816348$, $c_i = 0.0040752$. Normalization $\phi = 1 + 0i$ at $y = 1.5$ for the boundary layer and $R = 5000$, $\alpha = 2.7$, $c_r = 0.3486034$, $c_i = 0.0044436$. (The channel flow curves have been scaled up by 1000 for comparison) (here $\lambda = \lambda_1$).

One may now obtain $\tilde{r}_{ij}$ by subtracting (8) from (9),

$$\tilde{r}_{ij} = \varepsilon\tilde{s}_{ij} - \varepsilon\left(\frac{\lambda}{(\bar{u})'}\right)\left[\frac{1}{2}[\bar{\omega}_{ik}\tilde{s}_{kj} + \tilde{\omega}_{ik}\bar{s}_{kj} - \bar{s}_{ik}\tilde{\omega}_{kj} - \tilde{s}_{ik}\bar{\omega}_{kj}]\right]. \tag{10}$$

We next look at the stability equation corresponding to the organized disturbances. The mean flow is assumed to be parallel, or 'quasi-parallel', and two-dimensional. The disturbance equation (5) for $\tilde{u}_i$, with $\tilde{r}_{ij}$ given by (10), sets the framework for obtaining normal mode solutions. Two-dimensional disturbances are considered, and this leads to an extended form of the Orr-Sommerfeld equation, to be described later. Careful examination of the stability problem shows that the problem is not completely Squire-transformable. However it has been shown[19], that, for small obliqueness angle θ, the Squire transform is valid to within errors of $O(\theta^2)$. Thus, it is quite safe to base the analysis on two-dimensional disturbances. However, three-dimensional disturbances also need to be investigated for their own sake, in order to look at possible C-type resonant-triad interactions, and to look at longitudinal 'rolls', both of which could have a bearing on the spanwise organized structures seen in wall turbulent flows. Work on this aspect is going on.

To continue with the formulation, a streamfunction ψ is introduced for the organized disturbances such that $\tilde{u} = \partial\psi/\partial y$ and $\tilde{v} = -\partial\psi/\partial x$. After assuming normal modes, ψ may be expressed in the form

$$\psi = \phi(y)e^{i\alpha(x - ct)}, \tag{11}$$

where α is the spatial wave number and $c = c_r + ic_i$ is the (complex) wave speed. Introducing (11) in the evolution equation (5) for $\tilde{u}_i$, and remembering the quasi-parallel approximation for the mean flow and the closure equations for $\tilde{r}_{ij}$, one arrives at extended forms of the Orr-Sommerfeld equation, given below:

$$\begin{aligned} &i\alpha[(\bar{u}-c)(\phi'' - \alpha^2\phi) - \bar{u}''\phi] - 1/R[\phi'''' - 2\alpha^2\phi'' + \alpha^4\phi] \\ &\quad - 1/R[E\{\phi'''' - 2\alpha^2\phi'' + \alpha^4\phi\} + 2E'\{\phi''' - \alpha^2\phi'\} \\ &\quad + E''\{\phi'' + \alpha^2\phi\}] - \frac{\lambda E}{R}[-2i\alpha\phi''' + 2i\alpha^3\phi'] \\ &\quad - \frac{2i\alpha\phi'}{R}[\lambda E'' + 2\lambda' E' + \lambda'' E] = 0. \end{aligned} \tag{12}$$

Here primes denote differentiation with respect to y. All quantities in eq. (12) have been non-dimensionalised by outer variables. Also, in eq. (12), the first group terms in square brackets corresponds to the Rayleigh equation; the first two groups terms in square brackets correspond to the classical Orr-Sommerfeld equation; the remaining terms constitute the modifications to the Orr-Sommerfeld. Further, if $\lambda = 0$ in (12), the reduced equation thus obtained, is the same as the one derived by Reynolds and Hussain[8].

Incidentally, the unstable modes obtained (which will be discussed further later on) are wall modes which scale almost perfectly with inner variables. (Reynolds and Hussain[8] could not capture these modes); it is therefore instructive to express eq. (12) in inner variables. All quantities scaled with inner variables are superscripted by a '+' sign. The resulting equation becomes:

$$\begin{aligned} &i\alpha^+[(\bar{u}^+ - c^+)(\phi'' - \alpha^{+2}\phi) - \bar{u}^{+\prime\prime}\phi] - [\phi'''' - 2\alpha^{+2}\phi'' + \alpha^{+4}\phi] \\ &\quad - [E^+\{\phi'''' - 2\alpha^{+2}\phi'' + \alpha^{+4}\phi\} + 2E^{+\prime}\{\phi''' - \alpha^{+2}\phi'\} \\ &\quad + E^{+\prime\prime}\{\phi'' + \alpha^{+2}\phi\}] - \lambda^+E^+[-2i\alpha^+\phi''' + 2i\alpha^{+3}\phi'] \\ &\quad - 2i\alpha^+\phi'[\lambda^+E^{+\prime\prime} + 2\lambda^{+\prime}E^{+\prime} + \lambda^{+\prime\prime}E^+] = 0. \end{aligned} \tag{13}$$

The equation (13) is near universal for wall modes, because the Reynolds number becomes unity in inner variables, and only the eddy viscosity E has an outer dependence; but it has been seen by our present numerical calculations that wall modes are virtually confined to the wall region, which is why the answers are near universal.

A further point comes from the boundary conditions, which are the same as those for the classical Orr-Sommerfeld equation. The wall boundary conditions are the same for all cases, namely,

$$\phi,\ \phi' = 0 \text{ at } y = 0. \tag{14}$$

The outer boundary conditions for the different cases are as follows:

Boundary-layer flow:

$$\phi(y) \sim e^{-\alpha y}, \text{ for } y \to \infty. \tag{15a}$$

Channel flow centerline, symmetric mode:

$$\phi',\ \phi''' = 0, \text{ for } y = 1. \tag{15b}$$

Channel flow centerline, anti-symmetric mode:

$$\phi,\ \phi'' = 0, \text{ for } y = 1. \tag{15c}$$

The disturbance equation (12), along with the appropriate boundary conditions, constitutes an eigenvalue problem. In the temporal problem, α and R are chosen real and $c = c_r + ic_i$ is determined as the (complex) eigenvalue. Stability or instability is obtained respectively as $c_i < 0$ or $c_i > 0$.

The universality of the unstable inner modes was actually found *across different geometries*, i.e. virtually the *same* answers were obtained for boundary-layer flow, and for channel flow in *inner variables*, and the unstable range was found to be Reynolds number independent. This is because the classical $\phi \sim e^{-\alpha y}$ decay in the outer region sets in virtually from the *outer edge of the inner layer*. Thus, the eigenfunction becomes so small at the channel centerline/boundary-layer edge, that the *actual outer boundary condition has little influence on the inner modes*. However, *outer modes*, when these exist, are very much dependent on the outer boundary conditions.

Results and discussions

The numerical solutions of the extended Orr-Sommerfeld equation (12) were based on finite-difference methods developed in the earlier works of one of the authors[20,21]. In the present work the methods described in the earlier works for the stability of the Blasius boundary layer and laminar channel flow are extended to the present turbulent boundary layer and channel flow problem. The resolution used is ten times greater: the basic step size in y in the present problems is $h = 0.001$. Over a range of $0 \le y \le 1.5$, 1501 points are required for each array specification. Calculations have also been done using 15001 points. A seven-point finite difference scheme, employing a Noumerov transform and using a molecule described in Sen *et al.*[22], was employed in the calculations, and this gives a basic round-off accuracy of $O(h^6)$, i.e. 10^{-18} with $h = 0.001$. Thus all care was taken to ensure that the very rapid changes taking place in the inner region are faithfully taken into account in the numerical calculations. Also, the Blasius boundary layer results were verified as a cross-check. Calculations were performed using double precision arithmetic.

Typical eigenfunctions for the inner modes, in boundary layer and channel flow, are plotted in terms of $u_{\rm rms}$ and $v_{\rm rms}$ in Figure 3. Since the peaks are to arbitrary scale, dependent on the normalization adopted for ϕ, it is seen that the eigenfunctions are close to each other in shape. The same is also seen in Figure 4 for the plot of the production term $\tau_R(\bar{u})'$, where $\tau_R = \widetilde{\tilde{u}\tilde{v}}$. The shapes are similar for boundary layer flow and for channel flow when $\lambda = \lambda_1$ is used. However the shape is narrower for $\lambda = \lambda_3$. The peak of the curves is around $y^+ \approx 12.5$, which mimics the production peak in actual turbulence.

A wide range of numerical solutions was obtained for the extended Orr-Sommerfeld equation (12), for both boundary layer and channel flow, with R equal to 5000, 11000 and 17000. The results, plotted in inner variables, are shown in Figure 5 *a* for the case $\lambda = \lambda_1$. The notable feature in the results, which are for wall modes, is that the answers are essentially same despite different mean flow geometries. It is also seen that trends become nearly universal in the reported range of R as R becomes higher. Similar results are also shown, again

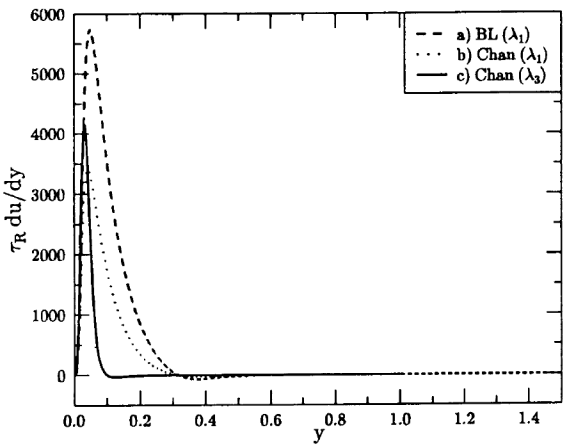

Figure 4. Graph of τ_R du/dy (production) versus y. a) Normalization $\phi = 1 + 0i$ at $y = 1.5$ for the boundary layer and $R = 5000$, $\alpha = 2.7$, $c_r = 0.3486034$, $c_i = 0.0044436$; b) Normalization, $\phi = 1 + 0i$ at $y = 1.0$ for channel flow and, $R = 5000$, $\alpha = 3.15$, $c_r = 0.3816348$, $c_i = 0.0040752$. [For curves (a) and (b), $\lambda = \lambda_1$]; c) Channel flow ($\lambda = \lambda_3$) and $R = 5000$, $\alpha = 9.434$, $c_r = 0.28762$, $c_i = 0.001693$ (vertical scale is arbitrary).

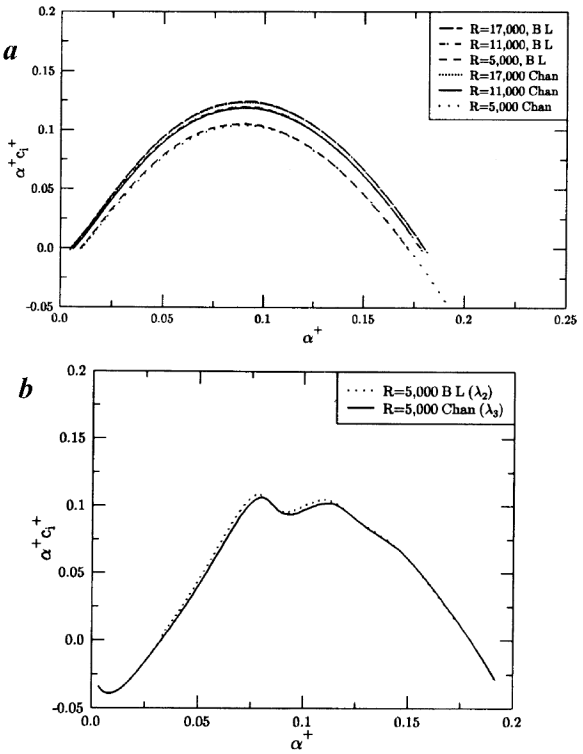

Figure 5. ***a***, Graph of the growth rate, $\alpha^+ c_i^+$ versus α^+, in inner scaling. (Here $\lambda = \lambda_1$ for all the curves.); ***b***, Graph of the growth rate, $\alpha^+ c_i^+$ versus α^+.

for wall modes, in Figure 5 *b*, but using λ_2 and λ_3. The results are essentially the same for all cases, and are qualitatively very close to the results for λ_1. It may also be seen in ref. 16 (Figure 12 therein), that the unstable range of α^+ is well contained within the energy-containing range of the actual measured turbulence spectrum.

The plot of an eigenfunction, in terms of u_{rms}, for an *outer mode* solution, is shown in Figure 6, using λ_3. It is indeed clear that these modes scale with outer variables and are spread over the whole range of y, unlike wall modes.

Some experiments have recently been performed to look for the existence of wall modes. A trip wire was set on the bottom wall of a wind tunnel, at the start of the test section, in order to generate a controlled turbulent boundary layer on the tunnel bottom wall. Organized disturbances were introduced into the bottom wall of the wind tunnel, through a 0.1 × 10 cm slot, using a speaker system. The frequency chosen was 400 Hz, which corresponds to about the peak growth rate in Figures 5 *a*, *b*. Measurements for the u velocity were now made downstream of the slot. By carrying out phase averaging of the raw turbulence signal, using the phase of the input sinusoidal disturbance as reference, the u_{rms} corresponding to the phase-averaged organized disturbance was obtained. This was carried out at different y stations, to obtain the distribution of u_{rms}. The result is shown in Figure 7. The shape of the distribution is in *very good agreement* with the theoretical results. In fact the value of α, and the Reynolds number R, corresponding to the experiments are respectively $\alpha \simeq 25$ and

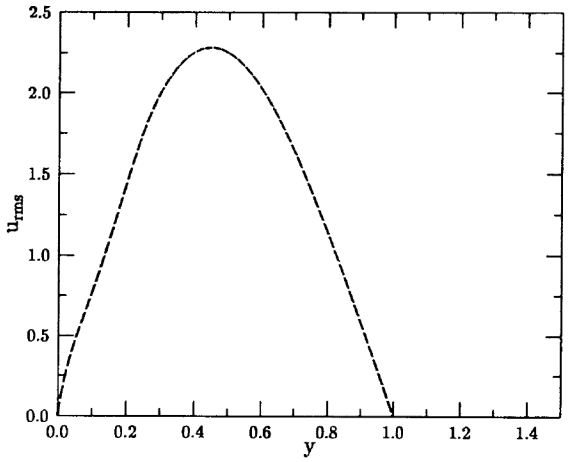

Figure 6. Graph of rms value of u versus y. Outer mode Normalization: $\phi = 1 + 0i$ at $y = 1.0$. $R = 12160$, $\alpha = 1.675$, $c_r = 1.02087$, $c_i = -0.02426$. (Here $\lambda = \lambda_3$.)

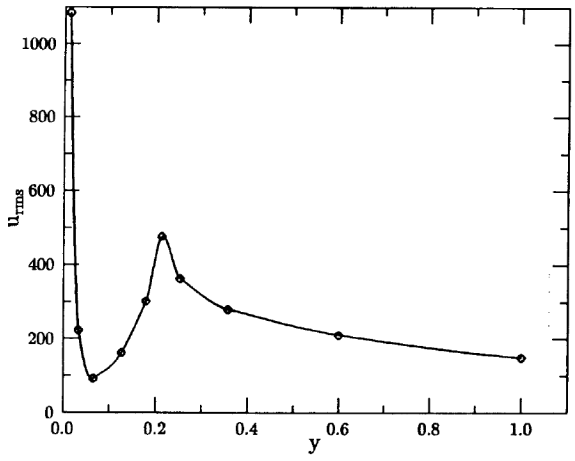

Figure 7. Graph of experimental data for u_{rms}, for the organized disturbance, versus y. Data corresponds approximately to $R = 5000$ and $\alpha = 25$. The scale for u_{rms} is in arbitrary units. The inner peak could not be obtained, since the data point obtained closest to wall is only 0.2 mm away from wall, corresponding to $y = 0.013$.

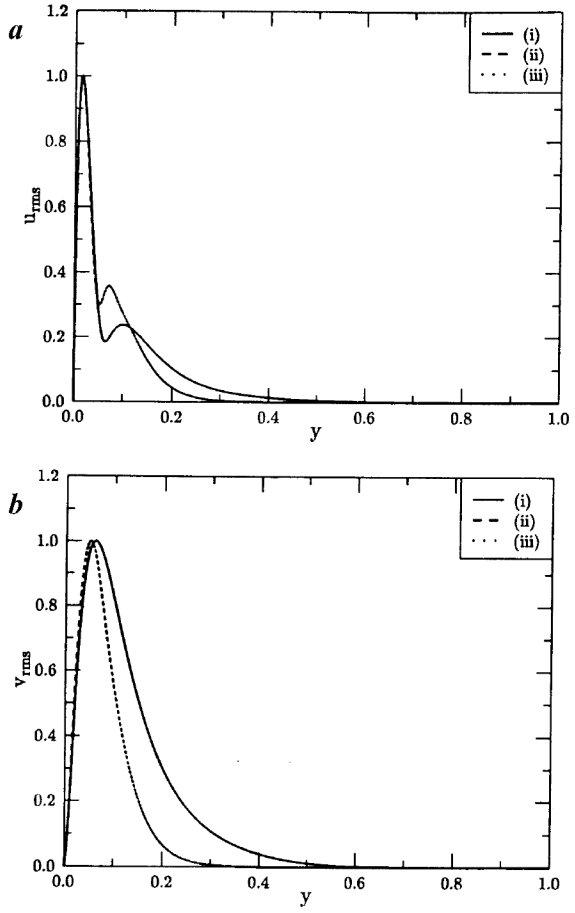

Figure 8. Graph of rms values of u versus y in the boundary layer. The Reynolds number is 5000 and the peaks have been normalized to 1 in all cases. ***a***, (i) $\alpha = 25.0$, $c_r = 0.33453$, $c_i = 0.054064$; $\lambda = \lambda_1$; (ii) $\alpha = 25.0$, $c_r = 0.316313$, $c_i = 0.05135$; $\lambda = \lambda_2$; (iii) $\alpha = 25.0$, $c_r = 0.316319$, $c_i = 0.051151$; $\lambda = \lambda_3$; ***b***, Graph of rms values of v versus y in the boundary layer.

$R \simeq 5000$. Figures 8 *a* and *b* respectively show numerically obtained plots for u_{rms} and v_{rms}, using all of λ_1, λ_2, λ_3, with $\alpha = 25$ and $R = 5000$. The plots for u_{rms} are in remarkably good agreement with the experiments, see Figure 7. Further, the outer peak of the u_{rms} curve in Figure 7 is further out as compared to the plots in Figure 8 *a*. *The experiments therefore provide some confirmation of the existence of wall modes, for organized disturbances introduced in turbulent flow*. A detailed paper on experiments will appear in future. It is possible that Hussain and Reynolds[9,10] could not get the wall modes in their experiments because they were looking at the wrong frequency values. Some discussion on this topic appears in Sen and Veeravalli[19].

Figure 8 *b* also shows the sharp $e^{-\alpha y}$ decay setting in at as low a value of y as $y \simeq 0.2$. This is the reason why the mean flow geometry has very little influence on the wall modes.

Conclusions

An extended Orr-Sommerfeld equation has been derived to accurately describe the evolution of organized disturbances in the presence of background turbulence. This has been done based on a few novel features in the formulation. First, it has been emphasized that the turbulent stresses in the problem can be suitably modelled based on the generalized eddy viscosity hypothesis. Second, after stipulating the validity of GEVH in the present problem, a *significant and logical* improvement has been made in modelling the Reynolds stress tensor, based on the generalized anisotropic formulation of Pope[12]. This improvement is also *unique* in form. Thirdly, in the formulation, the anisotropy is properly accounted for in terms of a universal non-dimensional function λ, which has been called the 'anisotropy function' herein. Fourthly, it is still reasonable to consider two-dimensional disturbances, because Squire's theorem is valid with error $O(\theta^2)$, where θ is the angle of oblique waves.

The numerical solution of the extended Orr-Sommerfeld equation (12) yielded unstable eigenvalues over a wide range of α. It has been found that instability is obtained by a large value of λ ($\simeq 9$ or more) in the wall region. However, the calculations are not sensitive to the exact shape of the λ-curve. The mode of instability obtained is the wall-mode, and the eigenfunction and the rms distributions of $\tilde{u}$ and $\tilde{v}$ are found to be qualitatively similar to those obtained for *Blasius* flow. Moreover, the locations of the respective peaks of the $\tilde{u}$ rms profile and the production term $\tau_R(\overline{u})'$, agree well with experimental values reported in literature, for *actual turbulence*. Thus the organized disturbances seem to mimic some of the features of actual turbulence.

The band of unstable eigenvalues, when scaled with respect to inner variables, indicates that results approach universality with high R. Particularly, the growth rate curves for different R in inner variables approach a limiting curve for high R, as may be seen in Figure 5 *a*. This is also a feature that correlates well with the inner scaling in actual turbulence.

The theoretical results also show the universality of wall modes, when scaled with respect to inner variables, across different mean-flow geometries. They also show the universality of the unstable range of frequencies. Essentially the same results are obtained for the wall modes, both for boundary layer and channel flow. However, the results for outer modes are different, and are dependent on the mean flow geometry. Outer modes are not important as they were all found to be damped.

Experiments reported in Sen and Veeravalli[16] have shown that the range of unstable frequencies, theoretically predicted, are well contained within the energy-containing range. Recent experiments are more revealing, and fully confirm the existence of the theoretically predicted wall modes. It is possible that Hussain and Reynolds[9,10] were not looking in the appropriate frequency range in their experiments, which is why they could not capture the wall modes, or obtained a mixture of wall and outer modes.

Three-dimensional spanwise structures, corresponding to C-type resonant triads, will be looked into as future work. Also, further experiments will go on for boundary layer flow, and in future, for channel flow.

As a final word in conclusion, it may be stated that the present work keeps alive the question of a possible connection between stability theory and actual turbulence in wall-bounded turbulent flows.

1. Gaster, M., Kit, E. and Wygnanski, I., *J. Fluid Mech.*, 1985, **150**, 23–39.
2. Liu, J. T. C., *Adv. Appl. Mech.*, 1988, **26**, 183–309.
3. Roshko, A., *Theoretical and Applied Mechanics* (eds Bodner, S. R., Singer, J., Solan, A. and Hussain, Z.), Elsevier Science, 1992.
4. Landau, L. D., *CR Acad. Sci. URSS*, 1944, **44**, 311–314.
5. Malkus, W. V. R., *J. Fluid Mech.*, 1956, **1**, 521.
6. Reynolds, W. C. and Tiederman, W. G., *J. Fluid Mech.*, 1967, **27**, 253–272.
7. Sen, P. K., Rakesh, G. A. and Veeravalli, S. V., Proceedings of the 20th National Conference on Fluid Mechanics and Fluid Power, Palghat, 1993, pp B3-1–B3-6.
8. Reynolds, W. C. and Hussain, A. K. M. F., *J. Fluid Mech*, 1972, **54**, 263–288.
9. Hussain, A. K. M. F. and Reynolds, W. C., *J. Fluid Mech.*, 1970, **41**, 241–258.
10. Hussain, A. K. M. F. and Reynolds, W. C., *J. Fluid Mech.*, 1972, **54**, 241–261.
11. Jang, P. S., Benney, D. J. and Gran, R. L., *J. Fluid Mech.*, 1986, **169**, 109–123.
12. Pope, S. B., *J. Fluid Mech.*, 1975, **72**, pp 331–340.
13. Sen, P. K. and Veeravalli, S. V., Proceedings of the 21st National Conference on Fluid Mechanics and Fluid Power, Osmania University, Hyderabad, 1994, pp TF-1–TF-6.

14. Sen, P. K. and Veeravalli, S. V., Proceedings of the 23rd National Conference on Fluid Mechanics and Fluid Power, MACT, 1996, Bhopal, pp 1–12.
15. Sen, P. K. and Veeravalli, S. V., Proceedings of the 23rd National Conference on Fluid Mechanics and Fluid Power, MACT, Bhopal, 1996, pp 13–18.
16. Sen, P. K. and Veeravalli, S. V., *Sadhana*, 1998, **23**, 167–193.
17. Sen, P. K. and Veeravalli, S. V., Proceedings of the 25th National Conference and 1st International Conference of FMFP, IIT Delhi, New Delhi, 1998, pp 853–860.
18. Sen, P. K. and Veeravalli, S. V., *J. Mech. Eng. Res. Dev.*, 1999, **21–22**, 81–89.
19. Sen, P. K. and Veeravalli, S. V., *Sadhana*, 2000, in press.
20. Sen, P. K. and Vashist, T. K., *Proc. R. Soc. London*, 1989, **424**, 81–92.
21. Sen, P. K., *Sadhana*, 1993, **18**, 387–403.
22. Sen, P. K., Venkateswarlu, D. and Maji, S., *J. Fluid Mech.*, 1985, **158**, 289–316.
23. Hussain, A. K. M. F. and Reynolds, W. C., *J. Fluids Engg.*, 1975, **97**, 568–578.

ACKNOWLEDGEMENTS. This project was funded by CSIR. We thank Dr Sukumar Mallick of CSIR for his logistic support from time to time. We also thank Mr Prashant Sarswat for his help in the measurements and data analysis. The cooperation of Mr T. R. Bhogal and the other staff of the Gas Dynamics Laboratory is also gratefully acknowledged. Finally, we offer grateful thanks to Professor R. Narasimha, for his constant encouragement, support and guidance.